Magnetoresistance Measurements of a Superconducting Surface State of In-Induced and Pb-Induced Structures on Si(111)

Manabu Yamada, Toru Hirahara,[*] and Shuji Hasegawa

Department of Physics, University of Tokyo, 7-3-1 Hongo, Bunkyo-ku, Tokyo 113-0033, Japan
(Received 6 June 2012; published 4 June 2013)

In situ micro-four-point-probe conductivity measurements in ultrahigh vacuum revealed that the Si(111)-striped incommensurate-Pb surface showed the superconductivity transition at 1.1 K. Both of the hexagonal and rectangular phases of Si(111)$\sqrt{7} \times \sqrt{3}$-In surface showed superconductivity at 2.4 and 2.8 K, respectively. By applying magnetic field perpendicular to the surface, the upper critical field was deduced to be 0.1–1 T. The derived Ginzburg-Landau coherence length of the Cooper pairs was several tens of nm, which was much smaller than the Pippard's coherence length estimated from the band structures. The short coherence length is determined by the carrier mean free path.

Surface superstructures formed on semiconductor substrates possess the surface states, which are inherently two dimensional (2D) and decoupled from the bulk. Using state-of-the-art techniques, it has now become possible to study the electronic transport phenomena in the surface states by conductivity measurements in ultrahigh vacuum [1–6] and describe the results from the band structures measured by angle-resolved photoemission spectroscopy [7]. Ultrathin metallic films grown on semiconductor substrates, especially superconducting ones, are also targets of active research of transport properties in relation to their structure and morphology [8–16]. However, there are no works that have performed magnetotransport measurements at subkelvin temperatures, which is likely needed to unravel the superconducting properties of surface superstructures.

Recently, Zhang *et al.* found by scanning tunneling spectroscopy (STS) that monolayers of In- and Pb-induced surface superstructures on Si(111), $\sqrt{7} \times \sqrt{3}$-In, $\sqrt{7} \times \sqrt{3}$-Pb, and striped incommensurate (SIC)-Pb phases, showed superconductivity at 1–3 K [17]. Uchihashi *et al.* followed by detecting the macroscopic superconducting current for $\sqrt{7} \times \sqrt{3}$-In [18]. These are the first examples of superconducting surface states. However, no conductivity measurements were done at such low temperatures with magnetic fields. Furthermore, although it has been known that there are both rectangular (rect) and hexagonal (hex) superstructures of the $\sqrt{7} \times \sqrt{3}$-In surfaces [19], previous studies failed to distinguish which phase is superconducting [17,18]. Since the transition temperatures reported were slightly different (3.1 K in Ref. [17] and 2.8 K in Ref. [18]), it may also be possible that both phases are superconducting with different transition temperatures.

In the present Letter, we have attempted to clarify the intriguing properties of these superconducting surface systems by performing *in situ* micro-four-point-probe (MFPP) resistance measurements down to 0.8 K under magnetic

fields up to 7 T. The Si(111)SIC-Pb surface is here shown to be superconducting by transport for the first time. Furthermore, we have made a clear distinction of the superconductivity of the hex- and rect-$\sqrt{7} \times \sqrt{3}$-In phases with transition temperatures of 2.4 and 2.8 K, respectively. Moreover, the superconducting coherence length of these surface systems is very short compared with that estimated from the surface-state band structures.

The measurements were performed *in situ* with our MFPP conductivity measurement system [20] in which the sample and MFPP was cooled down to 0.8 K and a magnetic field as high as 7 T was applied perpendicular to the surface. The probe spacing in MFPP was 20 μm [21]. The apparatus is also equipped with reflection high-energy electron diffraction (RHEED) for sample characterization. A clean Si(111)-7 × 7 surface was prepared by annealing an *n*-type substrate (P doped, 1–10 Ω cm at room temperature) by a cycle of resistive heat treatments. Then In or Pb was deposited at room temperature. The In coverage was calibrated by the formation of $\sqrt{3} \times \sqrt{3}$, $\sqrt{31} \times \sqrt{31}$, and 4 × 1 phases [6]. The $\sqrt{7} \times \sqrt{3}$-In surface was formed after 2.3–3.2 monolayer (ML) deposition followed by annealing at 430 °C for 2 s [6,18]. This surface superstructure was believed to contain In of 1–1.2 ML [19], but a recent theoretical calculation predicts nearly 2.4 ML [22]. The Pb coverage was calibrated by the formation of hexagonal-incommensurate and SIC phases [23]. The SIC-Pb surface was formed after 1.9 ML deposition, followed by annealing at 300 °C for 3 s [23–25]. The SIC phase is known to contain Pb of ∼1.3 ML [23]. By the annealing, the excess In or Pb atoms evaporate or make three-dimensional islands sparsely distributed on the surface. The RHEED patterns of the respective surfaces are shown in Fig. 1.

Figures 1(a) and 1(b) show the temperature dependence of the 2D sheet resistance for the $\sqrt{7} \times \sqrt{3}$-In (rect phase) and SIC-Pb surfaces, respectively. Both become a zero
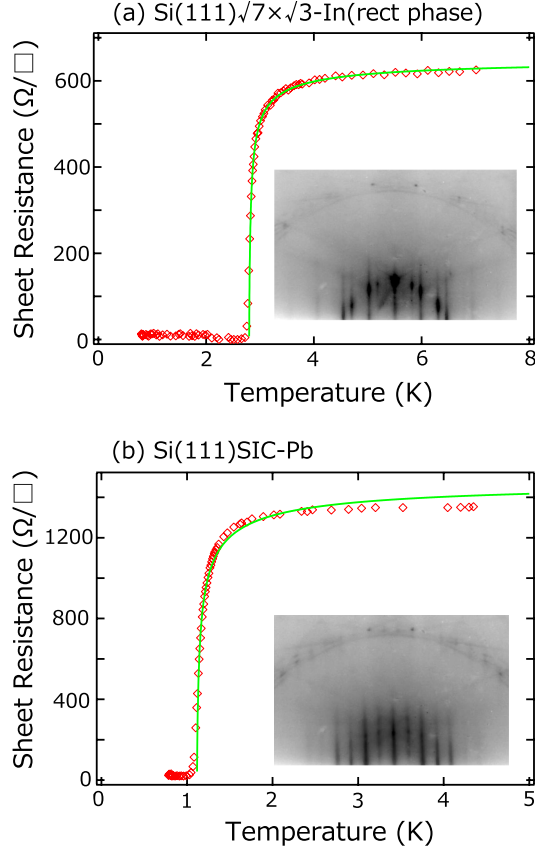
FIG. 1 (color online). Temperature dependence of the sheet resistance for the Si(111)$\sqrt{7} \times \sqrt{3}$-In (the rect phase) (a), and that of Si(111)SIC-Pb (b) surfaces, with the insets of RHEED patterns. The solid lines are results of the least-square fits to Eq. (1).

resistance state around 3 and 1 K, respectively. This is the first transport evidence of superconductivity for the Si(111) SIC-Pb surface.

In contrast to a sharp superconducting transition, the data in Fig. 1 show that the resistance starts to decrease above the superconducting transition temperature (T_c). This is due to the fluctuation conductivity in reduced dimensions since the present system is in the thickness of the atomic scale. There are several mechanisms that can lead to this correction [26]. Namely, they are (i) Aslamazov-Larkin conductivity due to the new conduction channel of the Cooper pairs above T_c (σ_{AL}), (ii) the decrease in conductivity due to the decrease of the one-electron density of state at the Fermi level (σ_{DOS}), and (iii) the Maki-Thompson contribution due to the coherent scattering of electrons forming a Cooper pair on the same elastic impurity (σ_{MT}). In σ_{MT}, there is a regular term $\sigma_{\text{MT}}^{\text{reg}}$ and an anomalous term $\sigma_{\text{MT}}^{\text{ano}}$. σ_{DOS} and $\sigma_{\text{MT}}^{\text{reg}}$ give nearly the same quantitative contribution to reduce the conductivity, whereas σ_{AL} and $\sigma_{\text{MT}}^{\text{ano}}$ increase the conductivity. Furthermore, it is known that σ_{DOS} and $\sigma_{\text{MT}}^{\text{reg}}$ give a much smaller correction for the in-plane conductivity and can be

neglected compared to σ_{AL} and $\sigma_{\text{MT}}^{\text{ano}}$ [26]. Therefore, the measured sheet resistance ρ above zero resistance can be fitted by

$$\rho = \frac{1}{\sigma_0 + \sigma_{\text{AL}} + \sigma_{\text{MT}}^{\text{ano}}}, \quad (1)$$

where σ_0 is the normal-state sheet conductivity. σ_{AL} and $\sigma_{\text{MT}}^{\text{ano}}$ are explicitly expressed as

$$\sigma_{\text{AL}} = \frac{e^2}{16\hbar} \frac{T_c}{T - T_c},$$

$$\sigma_{\text{MT}}^{\text{ano}} = \frac{e^2}{8\hbar} \frac{T_c}{T - (1 + \delta)T_c} \ln\frac{T - T_c}{\delta T_c}, \quad (2)$$

respectively, where δ is the "pair-breaking parameter" [27]. The solid lines in Figs. 1(a) and 1(b) are fitted curves which agree nicely with the experimental data. The T_c is thus determined to be 2.8 (a) and 1.1 K (b), respectively, [28]. δ is 0.19 (a) and 0.22 (b), which is in the same order of magnitude as that observed for Nb films [27].

For the $\sqrt{7} \times \sqrt{3}$-In surface, STS reported $T_c = 3.1$ K [17], while the previous conductivity measurements showed $T_c = 2.8$ K [18], in agreement with our result. For the SIC-Pb surface, $T_c = 1.8$ K by STS [17], while $T_c = 1.1$ K in Fig. 1(b). Thus conductivity measurements always show a lower T_c than that obtained by STS. This may be because the onset of superconductivity is very local due to fluctuations and can only be detected by STS, while the zero-resistance state can be realized when the fluctuation is suppressed at a lower temperature.

We have applied magnetic induction B in the surface-normal direction. Figures 2(a) and 2(d) show the sheet resistance at 0.8 K as a function of B for the $\sqrt{7} \times \sqrt{3}$-In (a) and SIC-Pb surfaces (d), respectively. The superconductivity is broken and finite resistance appears. Since it is difficult to precisely determine the upper critical field ($H_{c2} = B_{c2}/\mu_0$ where μ_0 is the magnetic permeability), we approximate it by the value linearly extrapolated to zero resistance in the ρ-B curves of Figs. 2(a) and 2(d). From the Ginzburg-Landau (GL) theory, H_{c2} can be related to the coherence length ξ_{GL} by

$$H_{c2}(T) = H_{c2}(0)\left(1 - \frac{T}{T_c}\right), \quad H_{c2}(0) = \frac{\phi_0}{2\pi\mu_0\xi_{\text{GL}}(0)^2}, \quad (3)$$

where $\xi_{\text{GL}}(0)$ is the GL coherence length at zero kelvin and ϕ_0 is the flux quantum [29]. Therefore, it is possible to estimate the coherence length $\xi_{\text{GL}}(0)$ from the temperature dependence of H_{c2}. Figures 2(b) and 2(e) show the resistance change with temperature under B. The superconducting transition is even more blurred by applying B. We have defined the "upper critical temperature" T_{c2} as an extrapolation of the linear part of decrease in resistance down to zero [30]. It is clear from Figs. 2(b) and 2(e) that T_{c2} becomes lower as the magnetic field is increased. In this
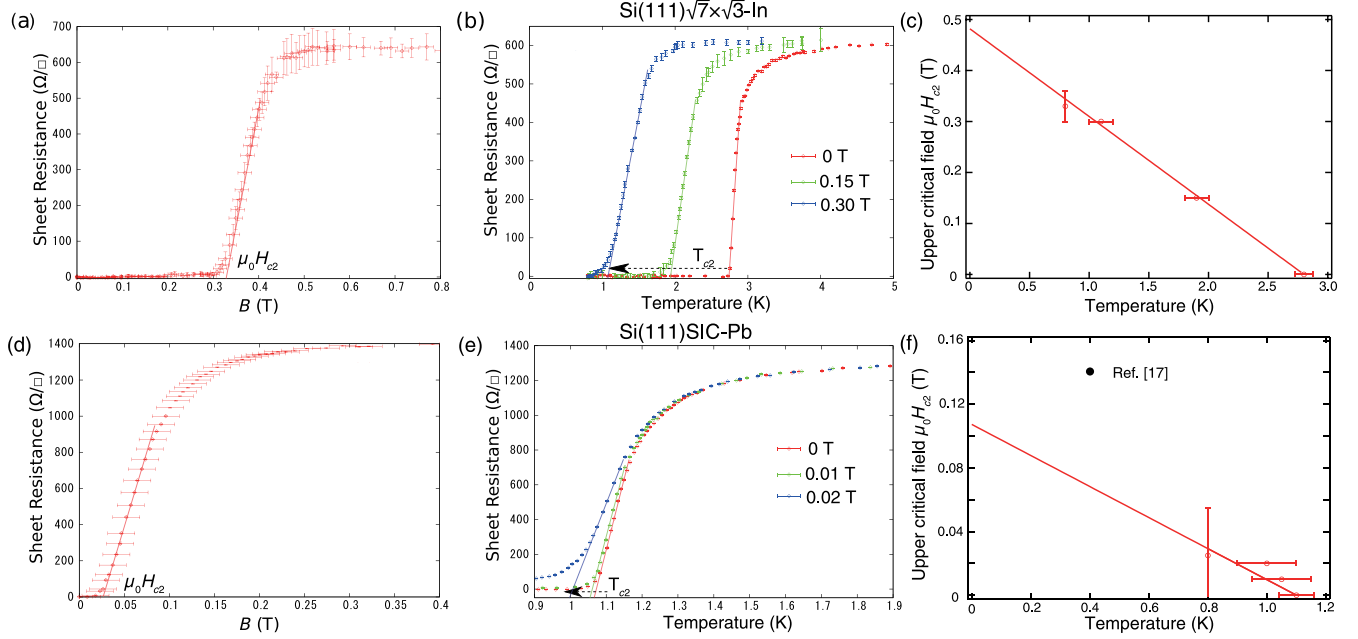
FIG. 2 (color online). (a)–(c) for Si(111)$\sqrt{7} \times \sqrt{3}$-In (rect phase), and (d)–(f) for Si(111)SIC-Pb surfaces, respectively. (a), (d) Magnetic field (B) dependence of the sheet resistance at 0.8 K. The solid lines show the extrapolation of the linear decreasing part of the resistance to zero resistance to determine $\mu_0 H_{c2}$. (b), (e) The change of the sheet resistance with temperature under different magnetic fields. The solid lines show the extrapolation of the linear decreasing part of the resistance to zero resistance to determine $Tc2$. (c), (f) The upper critical field as a function of temperature. The solid lines are the results of fitting to Eq. (3).

(B, T_{c2}) measurement, the applied magnetic field $H = B/\mu_0$ at temperature T_{c2} is regarded as the upper critical field H_{c2}. Figures 2(c) and 2(f) show such (H_{c2}, T) phase diagrams together with the data point of Figs. 2(a) and 2(d). The solid lines are results of least-square fitting to Eq. (3). The $\mu_0 H_{c2}(0)$ is 0.49 ± 0.02 T and 0.11 ± 0.03 T for the two surfaces, respectively. Accordingly, $\xi_{GL}(0)$ can be estimated to be 25 ± 7 nm and 74 ± 6 nm. The $\mu_0 H_{c2}$ estimated by STS in Ref. [17] for SIC-Pb is also shown in Fig. 2(f), which is roughly consistent with our data.

Now let us compare the present results with the band structure parameters obtained by angle-resolved photo-emission spectroscopy. From the BCS theory [29], there is another coherence parameter characterizing the super-conductivity called the Pippard's coherence length ξ_0, which is given by

$$\xi_0 = \frac{\hbar v_F}{\pi \Delta(0)} = \frac{2}{\pi} \left(\frac{k_B T_c}{2\Delta(0)} \right) \frac{\hbar^2 k_F}{m^* k_B T_c}, \quad (4)$$

where v_F is the Fermi velocity, $\Delta(0)$ is the gap size at zero kelvin, k_B is the Boltzmann constant, k_F is the Fermi wave number, and m^* is the effective mass. For the $\sqrt{7} \times \sqrt{3}$-In surface, $T_c = 2.8$ K, $k_F \sim 1.4$ Å^{-1}, $m^* \sim 1.1 m_e$ [31], and $2\Delta(0)/k_B T_c = 4.16$ [17] result in $\xi_0 \sim 610$ nm. For SIC-Pb, there is no reported value of k_F, but for the $\sqrt{7} \times \sqrt{3}$-Pb surface with less Pb coverage, $k_F \sim 1.36$ Å^{-1} and $m^* \sim 1.16 m_e$ [32]. Using these values, the same analysis gives $\xi_0 \sim 1.35\ \mu$m [$T_c = 1.1$ K and $2\Delta(0)/k_B T_c = 4.4$].

For pure materials at temperatures well below T_c, $\xi_{GL}(0) \approx \xi_0$ should hold [29]. But our analysis suggests $\xi_{GL}(0) \ll \xi_0$ for both surfaces, meaning that real Pippard's coherence length ξ must be rewritten as
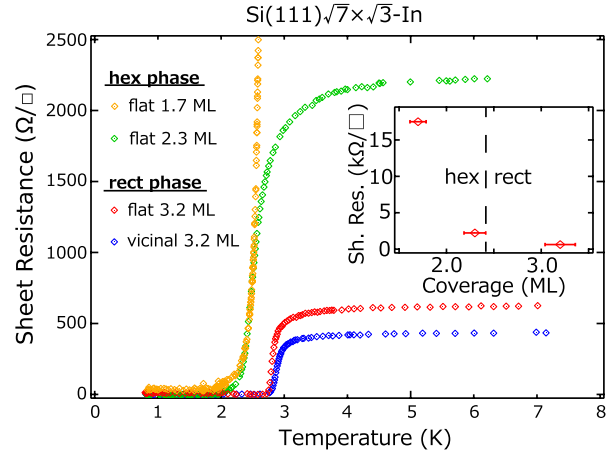

FIG. 3 (color online). Temperature dependence of the sheet resistance for the Si(111)$\sqrt{7} \times \sqrt{3}$-In surfaces formed by initial deposition of 3.2 ML-In on a flat substrate (red, slightly dark gray) and on a 0.9°-vicinal substrate (blue, charcoal gray), 2.3 ML-In (green, moderate gray) and 1.7 ML-In (orange, light gray) initial deposition on a flat substrate, respectively. All surfaces were flash heated at 430 °C to form the $\sqrt{7} \times \sqrt{3}$-In superstructure after room-temperature In deposition. The T_C is 2.8, 2.8, 2.4, and 2.4 K, respectively. The inset shows the normal-state sheet resistance as a function of the initial In coverage formed on a flat substrate.

TABLE I. Parameters of the superconductivity in Si(111)-$\sqrt{7}\times\sqrt{3}$-In and SIC-Pb surface superstructures. ρ_N is the resistance just above the superconducting transition. NA indicates data are not available since measurements were not performed.

Surface	Substrate	Coverage (ML)	ρ_N (Ω)	T_c (K)	$\mu_0 H_{c2}(0)$ (T)	$\xi_{GL}(0)$ (nm)	ξ_0 (nm)	Bulk T_c (K)	Bulk ξ (nm)
Hex-$\sqrt{7}\times\sqrt{3}$-In	Flat	1.7	17 500	2.4	NA	NA	610	3.41	250–440 [34]
		2.3	2200		1.0	19			
Rect-$\sqrt{7}\times\sqrt{3}$-In		3.2	610	2.8	0.49	25			
	0.9° vicinal	3.2	440		0.40	29			
SIC-Pb	Flat	1.9	1300	1.1	0.11	74	1350	7.20	83 [35]

$1/\xi = 1/\xi_0 + 1/l$, where l is the carrier mean free path in the system. Since $\xi_{GL}(0)$ should be close to ξ, our results suggest $\xi_{GL}(0) \sim l$ because $\xi_{GL}(0) \ll \xi_0$. This means that the coherence length is limited by the mean free path due to the presence of defects at the surface (atom vacancies, domain boundaries, etc.). In fact, the mean free path at the $\sqrt{7}\times\sqrt{3}$-In surface is $l \sim 10$ nm [6], on the same order of magnitude as $\xi_{GL}(0)$ estimated above. Since the sample prepared on a 0.9°-off vicinal surface shows lower normal-state resistance than that of the flat surface (Fig. 3, red and blue curves), we believe that not the steps but the defects within the terraces are the main source of carrier scattering [33]. Another possible reason for the small ξ_{GL} may be the intrinsically large fluctuation of the 2D super-conductivity [29].

We next discuss the difference between the hex and rect phases of the $\sqrt{7}\times\sqrt{3}$-In surface. We changed the Si substrate and the initial In coverages. Figure 3 shows the temperature dependence of the sheet resistance of the Si(111)$\sqrt{7}\times\sqrt{3}$-In surface formed by initial deposition of 3.2 ML In on a flat substrate [red, same as Fig. 1(a)], 3.2 ML In on a 0.9° vicinal substrate (blue), 2.3 ML In on a flat substrate (green), and 1.7 ML In on a flat substrate (orange). It can be recognized that the T_c for the lower In coverage surfaces (2.4 K) seems to be slightly lower than that of the 3.2 ML deposited surfaces (2.8 K). Considering the fact that a recent theoretical work suggests the coverage for the rect phase to be 2.4 ML [22], the surfaces with less In deposition should be the hex phase. Thus, Fig. 3 clearly shows that both the hex and rect phases show super-conductivity, but with different transition temperatures. The difference between the hex and rect phases can also be noticed in the RHEED pattern [36].

Table I summarizes the parameters obtained in the present study [37]. All the surfaces have the GL coherence length on the order of several tens of nm. The three data sets for the $\sqrt{7}\times\sqrt{3}$-In surface on a flat substrate show a tendency that the surface with a lower normal-state sheet resistance has a larger $\xi_{GL}(0)$. But they are still smaller than ξ_0 by an order of magnitude, meaning that ξ is determined by the mean free path. Thus the normal-state sheet resistance is closely related to the superconducting properties. In the inset of Fig. 3, we have shown the dependence of the normal-state sheet resistance on the initial In coverage. It decreases drastically with increasing In deposition. This is due to a transition from a phase mixed of hex and rect to the rect phase only; the domain boundaries in the mixed phase enhance the carrier scattering. In Figs. S1(a) and S1(b), the presence of the 4×1-In phase is clearly seen for the 1.3 and 1.7 ML deposited surfaces, while it disappears for 2.3 and 3.2 ML surfaces of (c) and (d) [36]. Thus, it seems that nearly 2 ML of In is needed to form the $\sqrt{7}\times\sqrt{3}$ periodicity over the whole surface. This actually suggests that the coverage for the hex-$\sqrt{7}\times\sqrt{3}$-In phase should be around 2 ML, consistent with Ref. [22].

In summary, we studied the superconducting properties of the Si(111)$\sqrt{7}\times\sqrt{3}$-In and SIC-Pb surfaces by the *in situ* MFPP method in ultrahigh vacuum down to 0.8 K with applying magnetic field up to 7 T. The T_c of the SIC-Pb surface was 1.1 K. We clearly distinguished the difference of T_c for the hexagonal (2.4 K) and rectangular (2.8 K) phases of $\sqrt{7}\times\sqrt{3}$-In. The values of $\mu_0 H_{c2}(0)$ was 0.1–1 T, and the deduced GL coherence length was several tens of nm. We have found that the superconducting co-herence length in the present systems is determined by the carrier mean free path, not by the intrinsic properties of the surface-state band structures.

---

*hirahara@surface.phys.s.u-tokyo.ac.jp

[1] T. Kanagawa, R. Hobara, I. Matsuda, T. Tanikawa, A. Natori, and S. Hasegawa, Phys. Rev. Lett. **91**, 036805 (2003).

[2] T. Tanikawa, I. Matsuda, T. Kanagawa, and S. Hasegawa, Phys. Rev. Lett. **93**, 016801 (2004).

[3] Ph. Hofmann and J. W. Wells, J. Phys. Condens. Matter **21**, 013003 (2009).

[4] C. Tegenkamp, Z. Kallassy, H. Pfnür, H. L. Günter, V. Zielasek, and M. Henzler, Phys. Rev. Lett. **95**, 176804 (2005).

[5] T. Uchihashi and U. Ramsperger, Appl. Phys. Lett. **80**, 4169 (2002).

[6] S. Yamazaki, Y. Hosomura, I. Matsuda, R. Hobara, T. Eguchi, Y. Hasegawa, and S. Hasegawa, Phys. Rev. Lett. **106,** 116802 (2011); I. Matsuda, C. Liu, T. Hirahara, M. Ueno, T. Tanikawa, T. Kanagawa, R. Hobara, S. Yamazaki, S. Hasegawa, and K. Kobayashi, Phys. Rev. Lett. **99,** 146805 (2007).

[7] I. Matsuda and S. Hasegawa, J. Phys. Condens. Matter **19,** 355007 (2007).

[8] O. Pfennigstorf, A. Petkova, H. L. Guenter, and M. Henzler, Phys. Rev. B **65,** 045412 (2002).

[9] N. Miyata, H. Narita, M. Ogawa, A. Harasawa, R. Hobara, T. Hirahara, P. Moras, D. Topwal, C. Carbone, S. Hasegawa, and I. Matsuda, Phys. Rev. B **83,** 195305 (2011).

[10] M. Jalochowski, E. Bauer, H. Knoppe, and G. Lilienkamp, Phys. Rev. B **45,** 13 607 (1992).

[11] O. Pfennigstorf, K. Lang, H.-L. Günter, and M. Henzler, Appl. Surf. Sci. **162–163,** 537 (2000).

[12] S. Qin, J. Kim, Q. Niu, and C.-K. Shih, Science **324,** 1314 (2009).

[13] M. Henzler, T. Lüer, and A. Burdach, Phys. Rev. B **58,** 10 046 (1998).

[14] M. Jałochowski, M. Hoffman, and E. Bauer, Phys. Rev. Lett. **76,** 4227 (1996).

[15] N. Miyata, R. Hobara, H. Narita, T. Hirahara, S. Hasegawa, and I. Matsuda, Jpn. J. Appl. Phys. **50,** 036602 (2011).

[16] H. Pfnür, D. Lükermann, and C. Tegenkamp, Phys. Status Solidi A **209,** 627 (2012).

[17] T. Zhang, P. Cheng, W.-J. Li, Y.-J. Sun, G. Wang, X.-G. Zhu, K. He, L. Wang, X. Ma, X. Chen, Y. Wang, Y. Liu, H.-Q. Lin, J.-F. Jia, and Q.-K. Xue, Nat. Phys. **6,** 104 (2010).

[18] T. Uchihashi, P. Mishra, M. Aono, and T. Nakayama, Phys. Rev. Lett. **107,** 207001 (2011).

[19] J. Kraft, M. G. Ramsey, and F. P. Netzer, Phys. Rev. B **55,** 5384 (1997).

[20] M. Yamada, T. Hirahara, R. Hobara, S. Hasegawa, H. Mizuno, Y. Miyatake, and T. Nagamura, e-J. Surf. Sci. Nanotechnol. **10,** 400 (2012).

[21] For details on the MFPP, see T. Tanikawa, I. Matsuda, R. Hobara, and S. Hasegawa, e-J. Surf. Sci. Nanotechnol. **1,** 50 (2003).

[22] J. W. Park and M. H. Kang, Phys. Rev. Lett. **109,** 166102 (2012).

[23] K. Horikoshi, X. Tong, T. Nagao, and S. Hasegawa, Phys. Rev. B **60,** 13 287 (1999).

[24] L. Seehofer, G. Falkenberg, D. Daboul, and R. L. Johnson, Phys. Rev. B **51,** 13 503 (1995).

[25] M. Hupalo, T. L. Chan, C. Z. Wang, K. M. Ho, and M. C. Tringides, Phys. Rev. B **66,** 161410(R) (2002); S. Stepanovsky, M. Yakes, V. Yeh, M. Hupalo, and M. C. Tringides, Surf. Sci. **600,** 1417 (2006).

[26] A. Larkin and A. Varlamov, *Theory of Fluctuations in Superconductors* (Oxford University, New York, 2005).

[27] J. W. P. Hsu and A. Kapitulnik, Phys. Rev. B **45,** 4819 (1992).

[28] There might also be some indications of a Kosterlitz-Thouless transition in the resistance-temperature curves close to T_c. The Kosterlitz-Thouless transition can be confirmed from current-voltage (IV) characteristics below T_c. However, we could not yet obtain reliable data because of limitations of accuracy in temperature control and the maximum current for measurements in our apparatus.

[29] M. Tinkham, *Introduction to Superconductivity* (Dover, New York, 1996).

[30] We believe that there is some uncertainty in determining the critical temperature in this way. The error bars in Figs. 2(c) and 2(f) show such uncertainty. However, the qualitative trend that T_{c2} decreases with increasing magnetic field is apparent in Figs. 2(b) and 2(e).

[31] E. Rotenberg, H. Koh, K. Rossnagel, H. W. Yeom, J. Schäfer, B. Krenzer, M. P. Rocha, and S. D. Kevan, Phys. Rev. Lett. **91,** 246404 (2003).

[32] W. H. Choi, H. Koh, E. Rotenberg, and H. W. Yeom, Phys. Rev. B **75,** 075329 (2007).

[33] The typical step-step distance on our sample was estimated to be 370 nm [18], which is much longer than the estimation of l. The average step-step distance on the 0.9°-off vicinal surface is about 20 nm. Therefore, if the steps are the main source of carrier scattering and determining the Cooper pair coherence, there should be significant influence on the measured conductivity and $\xi_{GL}(0)$. From Table I, this does not seem to be the case.

[34] R. D. Chandhari and J. B. Brown, Phys. Rev. **139,** A1482 (1965).

[35] C. Kittel, *Introduction to Solid State Physics* (John Wiley & Sons, New York, 1996), 7th ed.

[36] See Supplemental Material at http://link.aps.org/supplemental/10.1103/PhysRevLett.110.237001 for the RHEED patterns of the $\sqrt{7} \times \sqrt{3}$-In surface prepared at different initial In deposition.

[37] Since the band structure of the hex-$\sqrt{7} \times \sqrt{3}$-In surface is unknown, we have used the same parameters as the rect-$\sqrt{7} \times \sqrt{3}$-In. Thus, the values for the 2.3 ML data are only rough estimates.